

# SPECTRAL DISTRIBUTION OF THE DECAMETRIC RADIATION FROM JUPITER IN 1961

T. D. CARR, G. W. BROWN,\* AND A. G. SMITH

Department of Physics and Astronomy  
University of Florida, Gainesville, Florida

C. S. HIGGINS

Division of Radiophysics, C.S.I.R.O., Sydney, Australia

AND

H. BOLLHAGEN, J. MAY, AND J. LEVY

Maipu Radioastronomical Observatory  
University of Chile, Maipu, Chile

*Received April 4, 1964*

## ABSTRACT

Observations of the sporadic radiation from Jupiter were made in 1961 at observatories in Florida, in Australia, and in Chile, at various frequencies from 5 Mc/s to 85.5 Mc/s. A method was developed for computing the mean flux density for the apparition from measurements of peak flux density in consecutive 10-min intervals. Occurrence probability, peak flux density, and mean flux density for the apparition were determined as functions of frequency, and all three quantities were found to decrease monotonically with increase in frequency above 10 Mc/s. The decrease in mean flux density with increasing frequency indicated a spectral index in excess of 5.2 over much of the observed spectrum. Peak flux densities at 5 Mc/s and 10 Mc/s were about  $10^{-19} \text{ W m}^{-2}(\text{c/s})^{-1}$ . No activity was detected at 85.5 Mc/s. The ratio of mean flux density to peak flux density for 1-min intervals during noise storms was found to be essentially independent of frequency, suggesting that there is no appreciable change of noise-burst shape with frequency. The mean power emitted at decameter wavelengths by Jupiter in 1961 was estimated to be about  $5 \times 10^{10}$  watts, which is 1 or 2 orders of magnitude greater than that emitted at decimeter wavelengths. The average efficiency with which the solar-wind power incident on the Jovian magnetosphere is converted into decametric radiation power was estimated to be about  $10^{-5}$ . A rather large difference was observed in 10 Mc/s Jovian activity at the observatories in Australia and Chile, possibly due to a difference in scattering by field-aligned ionospheric irregularities at the two localities.

## I. INTRODUCTION

The noise which is received sporadically from Jupiter at decameter wavelengths exhibits complex spectral characteristics. It usually occurs in irregular bursts of 0.1–10 sec duration, the individual bursts occupying frequency bands of 0.5–2 Mc/s width (Smith, Carr, and Chatterton 1963). The center frequencies of successive bursts may be scattered over a band several magacycles wide. During the course of a noise storm, which is typically 10–60 min in duration, the active region of the spectrum may drift slowly either toward higher or lower frequencies (Carr, Smith, Bollhagen, Six, and Chatterton 1961; Warwick 1963).

The radiation has been reported at frequencies as low as 4.8 Mc/s (Ellis 1962) and as high as 38.5 Mc/s (Warwick 1963). Although considerable information can be found in the literature on the distribution of the noise in time, as e.g., the correlations of its occurrence with Jovian rotation and with solar activity, much less has been published on the variation of flux density and occurrence probability with frequency. Gardner and Shain (1958) gave  $10^{-19} \text{ W m}^{-2} (\text{c/s})^{-1}$  as the highest peak flux density recorded at 19.6 Mc/s, and somewhat less for both 27 Mc/s and 14 Mc/s. Kraus (1958) stated that flux densities of  $4 \times 10^{-22} \text{ W m}^{-2} (\text{c/s})^{-1}$  were commonly observed at 27 Mc/sec. Carr (1958) found from the early Florida measurements at 18 Mc/s that the  $5 \times 10^{-20} \text{ W m}^{-2} (\text{c/s})^{-1}$  level was exceeded on 11 per cent of the nights in 1957, while this value was exceeded on only 2 per cent of the nights in 1958. Ellis (1962) reported a peak flux

\* Now at Department of Physics, Union University, Jackson, Tennessee.

density of  $2 \times 10^{-20} \text{ W m}^{-2} (\text{c/s})^{-1}$  at 4.8 Mc/s, and an average value of  $10^{-22} \text{ W m}^{-2} (\text{c/s})^{-1}$  for all observed bursts (values which are not consistent with data presented later in the present report).

Carr *et al.* (1961) presented curves of occurrence probability as a function of frequency from 18 Mc/s to 27.6 Mc/s for the years 1958, 1959, and 1960, using data obtained in Florida and Chile. These curves decrease rapidly with increasing frequency above 18 Mc/s. The 1960 Chile data also included probability measurements at 16.7 Mc/s and 10 Mc/s, the probability at both of these frequencies being lower than at 18 Mc/s. Douglas and Smith (1963*a*) also measured the occurrence probability in 1960, at several frequencies from 16.5 Mc/s to 23 Mc/s. Their data suggest a maximum probability in the vicinity of 19 Mc/s, although the existence of a maximum is not proven by the data.

It is not possible to obtain a clear picture of the frequency dependence of flux density and occurrence probability from such fragmentary observations. However, it seems quite certain that both quantities decrease with increase in frequency above about 18 Mc/s. On the other hand, the suggested decrease in flux density and occurrence probability below 18 Mc/s (down to 4.8 Mc/s) has not been established. Measurement uncertainties in this region are much greater than at the higher frequencies because of more severe interference and ionospheric attenuation; the reported instances of a low-frequency dropoff are therefore subject to question. The results presented in this paper help to clarify some of the questions regarding the spectral distribution of noise bursts from Jupiter above 5 Mc/s.

## II. OBSERVATIONS AND EQUIPMENT

During the 1961 apparition of Jupiter, radio observations were made each night at the University of Florida Radio Observatory near Gainesville, Florida, and at the Maipu Radioastronomical Observatory near Santiago, Chile. Several frequencies ranging from 5 Mc/s to 31 Mc/s were monitored. During part of this time, observations were also made at the Fleurs Field Station of the Radiophysics Laboratory, near Sydney, Australia, at 10 Mc/s, 19.7 Mc/s, and 85.5 Mc/s.

Thirteen fixed-frequency channels were monitored at the three observatories. An operator was always present at each station when recordings were being made. The chief duty of the operator was to identify all interference and to make the appropriate notations on the records. The only channel which was not closely watched was that at 85.5 Mc/s. Interference at this frequency was recognizable by the deflection of the recorder pen of a second 85.5 Mc/s radiometer having an essentially non-directional antenna; interference on this second radiometer was always more intense than on the one monitoring Jupiter. The channel locations, antenna types, and observing periods are summarized in Table 1.

The 85.5 Mc/s and 19.7 Mc/s arrays were much larger than the others, as can be seen from Table 1. The 85.5 Mc/s array was a portion of the north-south arm of the original Mills Cross (Mills, Little, Sheridan, and Slee 1958). The 19.7 Mc/s antenna was a portion of the north-south arm of the cross array built by Shain (1958). The receiver band widths were about 4 kc/s for all channels except the one at 85.5 Mc/s, for which the band width was about 250 kc/s. The pen recorders were normally operated at paper speeds of about 6 inches/hour, with time constants somewhat less than 1 sec. Supplementary recorders having higher paper speeds and shorter time constants were used occasionally for better resolution of individual bursts.

## III. OCCURRENCE PROBABILITIES

The numbers of nights of effective monitoring on the various channels are listed in Table 1. The probability of occurrence of detectable radiation from Jupiter for the entire season was calculated for each channel by dividing the total number of hours of

Jupiter activity by the total number of hours of effective monitoring. Only the periods during which radiation from Jupiter could have been detected if it had been present were included in the effective monitoring time; portions of records on which interference was excessive were rejected. The results are shown in Figure 1 for all channels listed in Table 1 except the 5 Mc/s channel in Chile and the 85.5, 19.7, and 10 Mc/s channels in Australia. Although the occurrence probability is known to be strongly correlated with the System III longitude of the central meridian at the time of occurrence (Carr *et al.* 1961), this effect did not influence the results presented in Figure 1, because on each channel all central meridian longitudes were monitored almost equally. It has also

TABLE 1  
ANTENNA DATA AND OBSERVATION DATES

Frequency (Mc/s)	Station*	Type of Array	Observing Time per Night (hours)	Observing Period (1961)	Nights Monitored	Period of Flux Measurements (1961)
5	C	2-dipole ( $\lambda/2$ ) broadside, fixed on meridian	4	Apr 13–Aug. 17	8	0
10	A	4-dipole ( $\lambda/2$ ) broadside, phase-steered	7	June 19–Aug. 31	71	June 19–Aug 31
10	C	4-dipole ( $\lambda/2$ ) broadside, phase-steered	7	Mar. 4–Sept. 13	179	June 2–Aug 29
15	C	4-dipole ( $\lambda/2$ ) broadside, phase-steered	7	Mar. 18–Nov. 1	178	June 2–Aug. 30
18	F	5-element steerable yagi	8	Feb. 2, 1961– Feb. 1, 1962	341	0
18	C	Interferometer; 2 phase-steered 8-dipole ( $\lambda/2$ ) broadsides	7	Feb. 10–Nov 20	274	June 2–Aug 31
19.7	A	43-dipole ( $\lambda/2$ ) N.–S linear array, partially phase-steered	6	June 19–Aug. 31	71	June 19–Aug 31
20	C	8-dipole ( $\lambda/2$ ) broadside, phase-steered	7	Mar. 7–Nov. 20	230	June 2–Aug 31
22.2	F	Pair of crossed 4-element yagis, fixed on meridian	4	Feb. 26–Nov. 28	254	0
22.2	C	Two 2-dipole ( $\lambda/2$ ) broadsides, mutually perpendicular; fixed on meridian	4	Mar. 7–Nov. 20	249	0
27.6	F	7-element steerable yagi	8	Feb. 1, 1961– Jan. 31, 1962	327	Aug 20–Nov 13
31	F	$\lambda/2$ -dipole in corner reflector, fixed on meridian	4	June 8–Oct. 25	136	0
85.5	A	75-dipole ( $\lambda$ ) N.–S linear array	$2\frac{1}{4}$	July 3–July 31	28	July 3–July 31

\* "C" refers to Chile, "A" to Australia, and "F" to Florida.

been shown that the occurrence probability is correlated with Jovian elongation, being greatest at opposition (Douglas 1960; Six 1962). Since the median observing dates for the various channels differed somewhat, the occurrence probabilities presented in Figure 1 may have been influenced by the elongation effect. However, it is believed that these errors are relatively small. Occurrence probabilities for the years 1958, 1959, and 1960 (Carr *et al.* 1961) are also included in Figure 1 for comparison with the 1961 probabilities. The 1961 curve is higher than those for the preceding years. This is consistent with the inverse relationship between occurrence probability and solar activity reported by Carr *et al.* It is interesting to note that the 1961 data indicate a monotonic increase in occurrence probability with decrease in frequency down to 10 Mc/s, the lowest frequency plotted, rather than a maximum in the vicinity of 18 Mc/s. It now seems likely

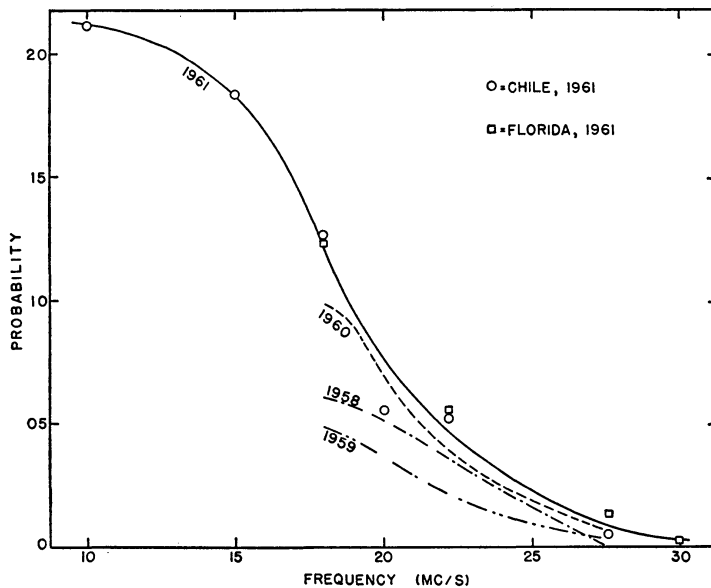


FIG. 1.—Probability of occurrence of radiation from Jupiter at the observatories in Florida and Chile in 1961 as a function of frequency. Previously published curves for 1958, 1959, and 1960 are included for comparison (the portion of the 1960 curve below 18 Mc/s having been omitted).

that the apparent maximum in the 1960 curve was not real, but may have resulted from ionospheric effects. One would expect such effects to be less pronounced in 1961 than in 1960 because of the improved ionospheric conditions accompanying decreasing solar activity.

Of the four channels which were omitted from the 1961 curve in Figure 1, 5 Mc/s was not included because of insufficient data, 85.5 Mc/s because the observed probability was zero, and the 10 Mc/s and 19.7 Mc/s Australia channels because the probabilities were much higher than for the corresponding channels in Chile and in Florida. Occurrence probabilities for corresponding Australian and Chilean observations are compared in Table 2. Only those Chilean observations which were made during the same period as the Australian observations were used in the probability determinations for Table 2, and therefore the Chilean probabilities in this case are slightly different from those in Figure 1.

The significantly higher probability at 19.7 Mc/s in Australia than at 18 Mc/s or 20 Mc/s in Chile can perhaps be attributed to the fact that the 19.7 Mc/s antenna was of unusually high directivity, permitting the detection of weaker signals. However, the higher probability at 10 Mc/s in Australia than in Chile cannot be explained in this

way. The two antennas at this frequency were almost identical, and the same operating techniques were employed at the two stations (one of the observers spent parts of the apparition at both places). The stations are at very nearly the same geographic latitude, although their geomagnetic latitudes are quite different. It is suggested that the observed difference in occurrence probabilities at 10 Mc/s resulted from a greater transparency of the ionosphere at the Australian station than at the one in Chile. The F-layer critical frequencies at the two locations were usually very nearly the same at corresponding local times, and were considerably below 10 Mc/s. (The monthly median ordinary-wave critical frequencies for July and August at both stations during the hours of observation were usually below 4 Mc/s, and almost always below 5 Mc/s.) It is tempting to speculate that the observed difference might have been related in some way to the difference in direction of the geomagnetic field with respect to the ray path in the ionosphere at the two localities. The line of sight to Jupiter intersected

TABLE 2  
COMPARISON OF OCCURRENCE PROBABILITIES AT THE CHILEAN AND AUSTRALIAN STATIONS, JUNE 19 TO AUGUST 31, 1961

STATION	OCCURRENCE PROBABILITY			
	At 10 Mc/s	At 18 Mc/s	At 19.7 Mc/s	At 20 Mc/s
Chile	0 21	0 14	0 19	0 045
Australia	0 46	..	..	..

the geomagnetic field at  $47^\circ$  at the Chilean station at transit, while the corresponding angle at the Australian station was only  $11^\circ$ . Perhaps some of the incident radiation was scattered by field-aligned ionospheric irregularities, the amount of the scattering being the less, the more nearly parallel the rays were to the field.

#### IV. FLUX DENSITY CALIBRATION

For each channel, the flux density corresponding to a given Jupiter noise deflection was determined from the effective area of the antenna, the power sensitivity of the receiver-recorder combination, and the background deflection which was due largely to galactic noise. The effective area of the 85.5 Mc/s array was found from observations of previously calibrated discrete sources. That of the 19.7 Mc/s array was measured by comparing solar bursts received simultaneously with the array and with a standard dipole. The manufacturer's measured gain values were used to calculate the effective areas of the 18 Mc/s and the 27.6 Mc/s yagis at the Florida observatory. The assumed effective areas of the other antennas were based on data derived from handbooks. Calibration steps were put on most of the records; they were produced by temperature-limited noise diodes which were connected to the receiver inputs in place of the antennas. All recorder deflections could thus be converted into corresponding values of power per unit band width. The power per unit band width due to a signal from Jupiter was found by taking the difference between the values corresponding to the total deflection and to the undisturbed background level.

On several of the channels, the galactic background was used as an auxiliary calibration for those records not having noise-diode calibrations. The averages of the calibrator currents which produced the same deflections as the nightly mean galactic deflections are listed in Table 3 for the nights on which noise-diode calibrations were made on these channels. The standard deviations indicate the spread of the nightly mean galactic levels about the average for the apparition. The relatively large standard deviations at

10 Mc/s were probably due to night-to-night fluctuations in the width of the cone of galactic radiation emerging from the ionosphere toward the antenna. The angular width of this cone is dependent on the ionospheric critical frequency. The errors in average Jupiter flux density at 10 Mc/s due to this fluctuation probably did not exceed 30 per cent, and were undoubtedly much smaller at the higher frequencies.

#### V. PEAK FLUX DENSITIES

The maximum value of flux density attained on each frequency during the apparition can be used as a rough measure of the relative intensity of the Jupiter noise during the active periods on that frequency. Although such an intensity measure is admittedly crude in comparison with the more refined method to be presented in the next section, it has the advantage of simplicity, and it seems to give consistent results. Rather than relying on a single maximum, it was decided to use the average of the five highest

TABLE 3  
MEANS OF THE NIGHTLY AVERAGE GALACTIC  
LEVELS, EXPRESSED IN EQUIVALENT  
CALIBRATOR CURRENT

Frequency (Mc/s)	Station	Equivalent Calibrator Current (ma)	Standard Deviation (ma)
10	Australia	528	309
10	Chile	361	107
15	Chile	221	33
18	Chile	91	19
20	Chile	84	19
27 6	Florida	15	3

nightly maximum flux densities on each frequency. These averages are plotted as a function of frequency in Figure 2. As in the case of the occurrence probability, the averaged peak flux density increases monotonically with decreasing frequency down to 10 Mc/s. The value originally obtained at 5 Mc/s was considered uncertain because of calibration difficulties and the scarcity of interference-free records in 1961. Nevertheless, it agreed to within a factor of 2 with the corresponding 1962 value for 5 Mc/s, for which good records were abundant and calibrations were more reliable. The 5 Mc/s point shown in Figure 2 is the one for 1962; all the others are for 1961. The curve of Figure 2 suggests that the averaged peak flux density is a maximum in the vicinity of 10 Mc/s; however, a dropoff at 5 Mc/s is by no means certain. The averaged peak flux densities at 5 Mc/s for 1961 and 1962 were between  $10^{-19}$  and  $10^{-18}$   $\text{W m}^{-2} (\text{c/s})^{-1}$ ; Ellis (1962) reported a peak value of  $2 \times 10^{-20}$   $\text{W m}^{-2} (\text{c/s})^{-1}$  at 4.8 Mc/s during 1961. The reason for this discrepancy is not known.

No radiation from Jupiter was observed at 85.5 Mc/s; if there had been any in excess of  $5 \times 10^{-25}$   $\text{W m}^{-2} (\text{c/s})^{-1}$ , it would have been detected. This detection sensitivity level is indicated in Figure 2. The 85.5 Mc/s data were provided by Bruce Slee of the C.S.I.R.O. Radiophysics Laboratory at Sydney. Mr. Slee also observed Jupiter at 85.5 Mc/s in 1960, with negative results. The 1960 observations were for 33 nights at  $2\frac{1}{4}$  hours per night, with the same detection sensitivity as in 1961.

#### VI. METHOD OF DETERMINING MEAN FLUX DENSITY

The mean flux density for each frequency is probably a more significant quantity than the peak value, but it is much more difficult to determine. If one knew the proba-

bility that any given flux density is exceeded, the mean value could be calculated. However, the labor involved in preparing such probability distribution functions from an analysis of all the data would be prohibitive. Moreover, since it would be necessary to run the recorders fast enough to resolve the individual noise bursts, an unmanageable bulk of records would result. These difficulties were circumvented by the development of a data reduction scheme based upon systematic sampling. The following symbols will be used in describing the method:

$S$  = peak flux density in one 10-minute interval

$\langle S \rangle_1$  = mean flux density during one interval

$\langle S \rangle_a$  = mean flux density for the entire apparition

$N$  = total number of intervals observed during apparition

$f(S)dS$  = fraction of intervals for which the peak flux density lies between  $S$  and  $S + dS$

$F(S)$  = fraction of intervals for which the peak flux density equals or exceeds  $S$

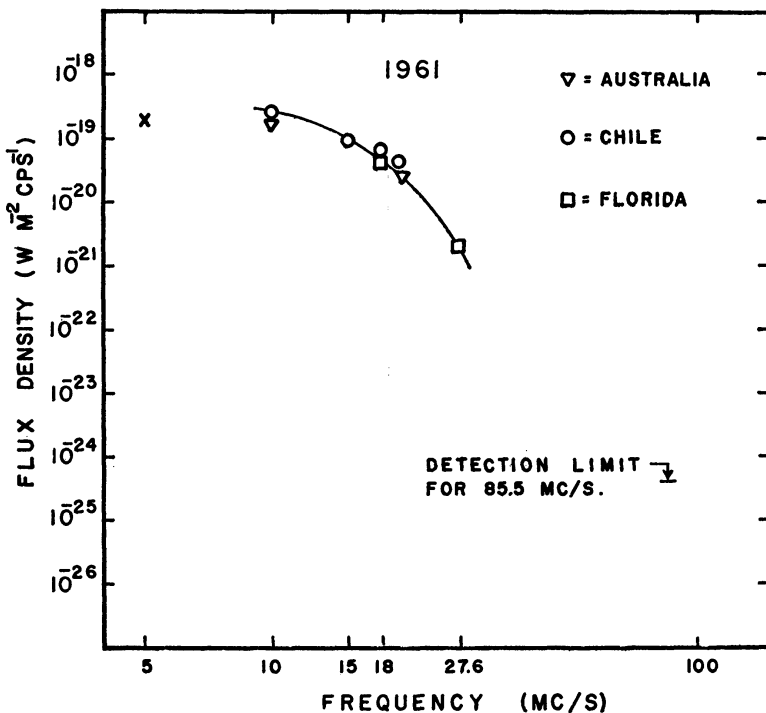


FIG. 2.—Means of the five nightly maximum peak flux densities of the radiation from Jupiter at three observatories in 1961 as a function of frequency. The point marked  $X$  is the value for the 5 Mc/s channel in Chile in 1962. The detection limit at 85.5 Mc/s is indicated, although the radiation was not received at this frequency.

All records were divided into consecutive 10-min intervals, and the flux density of the highest peak in each interval was measured. For each channel, the fraction  $F(S)$  of the intervals for which the peak flux density equaled or exceeded each of a number of different values of  $S$  was found, and this fraction was plotted as a function of  $S$ . It was then assumed that, on the average, the mean flux density in each interval is proportional to the peak flux density in that interval, or

$$\langle S \rangle_1 = KS, \quad (1)$$

where  $K$  is the constant of proportionality. Tests described in a later section indicated that this assumption is valid, and that the same value of  $K$  can be used for the entire range of frequencies. The mean flux density for the apparition is given by

$$\langle S \rangle_a = \frac{1}{N} \sum_{j=1}^{j=N} (\langle S \rangle_1)_j. \quad (2)$$

Thus,

$$\langle S \rangle_a = \frac{K}{N} \sum_{j=1}^{j=N} S_j = K \int_0^{\infty} S f(S) dS. \quad (3)$$

But it is easily shown that

$$f(S) = -\frac{d}{dS} F(S), \quad (4)$$

so that

$$\langle S \rangle_a = K \int_0^1 S dF(S) = K \int_0^{\infty} F(S) dS. \quad (5)$$

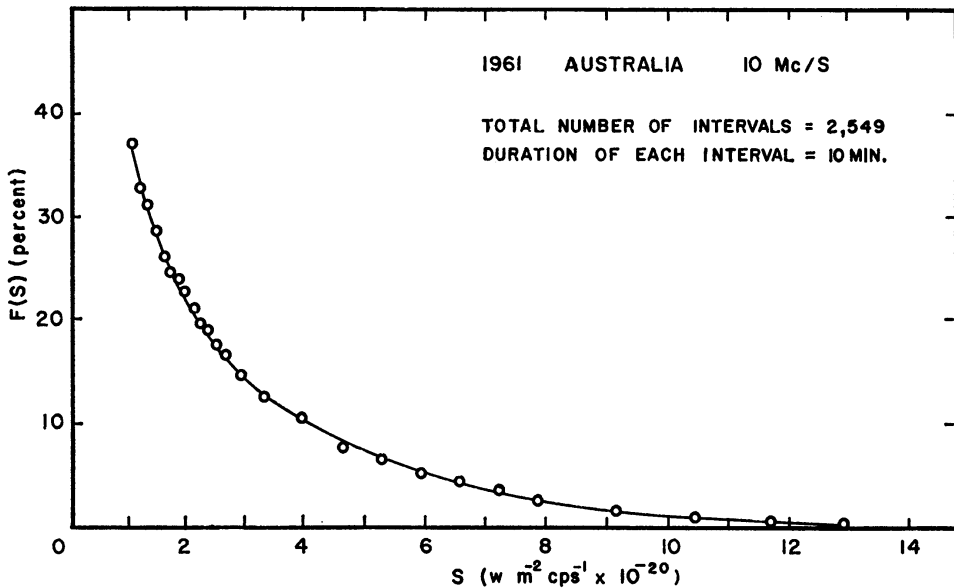


FIG. 3.—Probability distribution function for the peak flux densities in consecutive 10-min intervals, 10 Mc/s in Australia.

Therefore, the mean flux density for the apparition can be obtained from the distribution function  $F(S)$  and the average ratio of mean to peak flux density in the 10-min intervals.

#### VII. THE DISTRIBUTION FUNCTIONS

The distribution functions  $F(S)$  for the data from the various calibrated channels are presented in Figures 3–9. The number of 10-min intervals used in compiling  $F(S)$  is given in each figure. The beginning and ending dates for the periods during which these data were obtained are listed in the last column of Table 1. All of the functions  $F(S)$  are presented together on a semilog plot in Figure 10. It is interesting to note that each curve in Figure 10 is very nearly a straight line except at its high flux-density end. The low flux-density ends of the curves could not be resolved because of back-



ground-noise fluctuations. The 10 Mc/s and 19.7 Mc/s curves from the Australian station are higher than the curves for similar frequencies from the Chilean station. That this is due to the more frequent reception of Jovian noise at the Australian station, rather than to its being of higher intensity when it is received, is indicated by Table 2 and Figure 2.

Figure 11 is a plot of the flux density which is exceeded in 3 per cent of the 10-min intervals as a function of frequency. A similar curve for any higher percentage would of course lie below the 3 per cent curve.

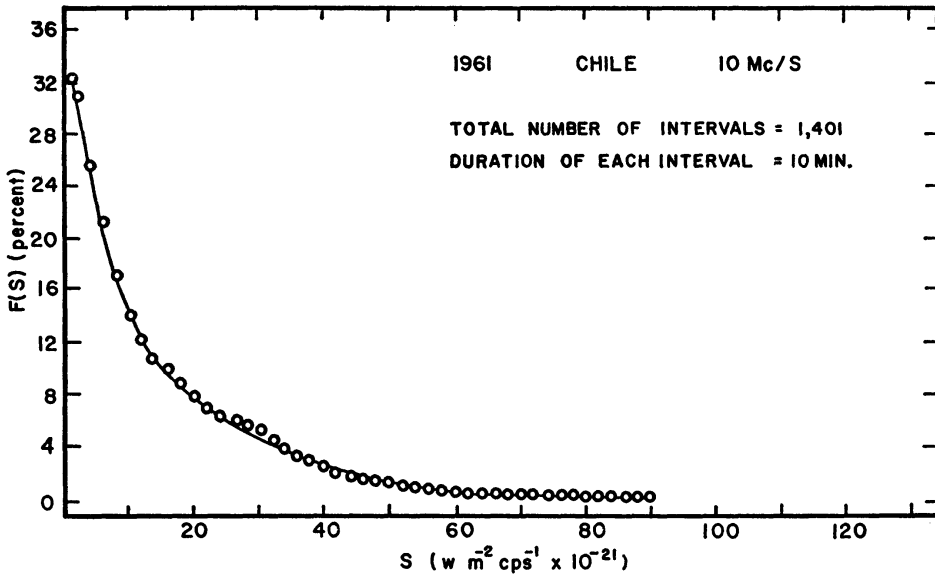


FIG. 4.—Probability distribution function for the peak flux densities in consecutive 10-min intervals, 10 Mc/s in Chile.

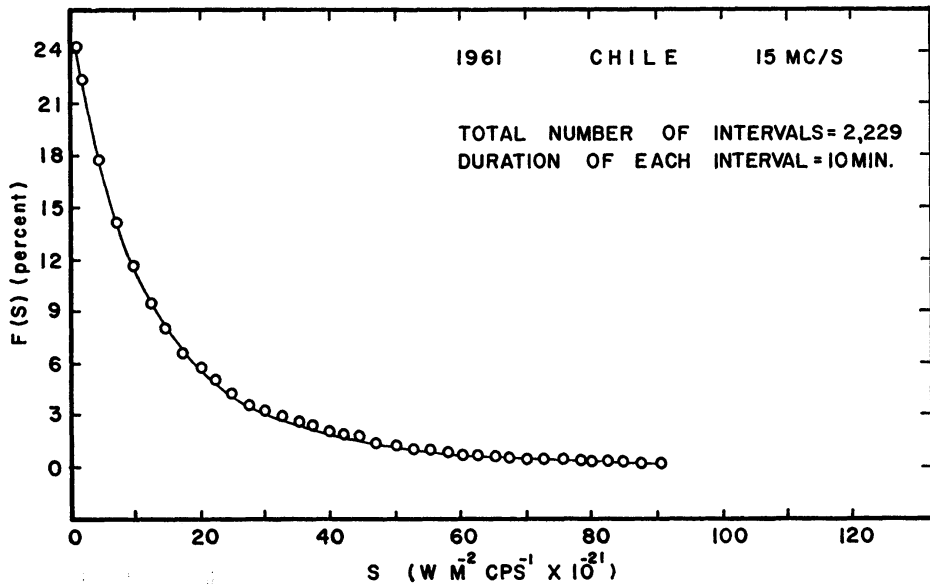


FIG. 5.—Probability distribution function for the peak flux densities in consecutive 10-min intervals, 15 Mc/s in Chile.

## VIII. THE RATIO OF MEAN TO PEAK FLUX DENSITY

It was necessary to establish the fact that the ratio  $\langle S \rangle_1 / S$ , i.e.,  $K$ , approaches a constant when it is averaged over a sufficiently large number of intervals, and to determine the value of this constant for each frequency. Pen recordings made at a paper speed of 5 mm/sec, which is fast enough to resolve the individual Jovian noise bursts, were used in the determination of  $K$ . The following additional symbols will be employed

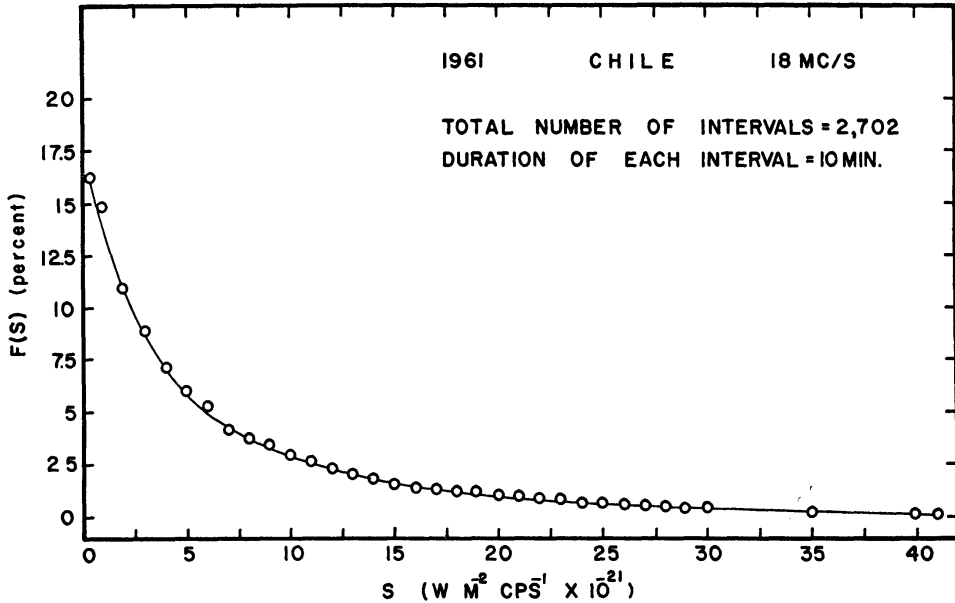


FIG. 6.—Probability distribution function for the peak flux densities in consecutive 10-min intervals, 18 Mc/s in Chile.

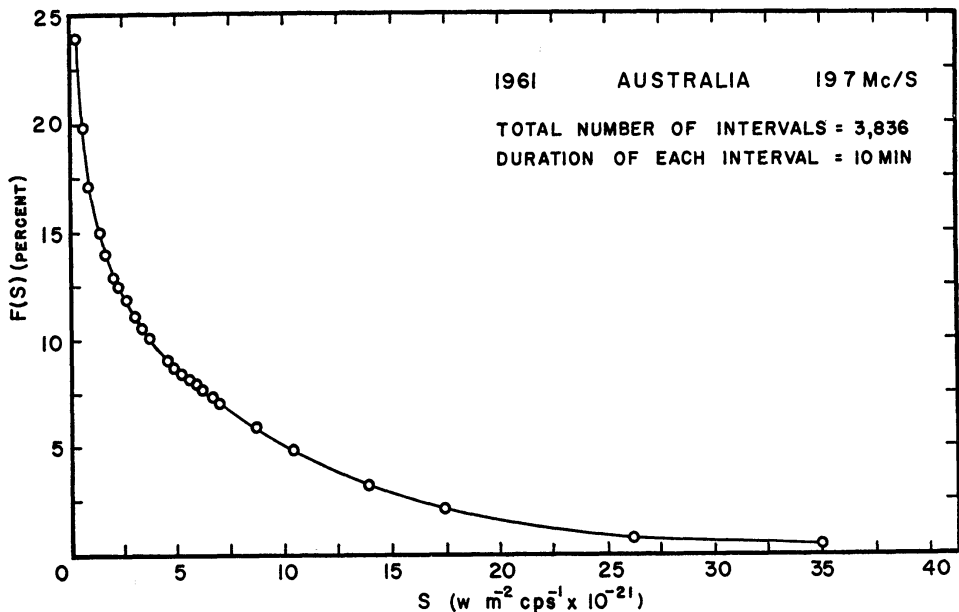


FIG. 7.—Probability distribution function for the peak flux densities in consecutive 10-min intervals, 19.7 Mc/s in Australia.

in the derivation of the expression for  $K$  for a given interval in terms of deflections measured from the record:

$x$  = pen deflection

$x_0$  = pen deflection due to galactic background

$x_1$  = deflection due to highest peak in selected interval

$C$  = calibration constant for receiving-recording system

$T$  = duration of the selected interval

$t$  = time that the deflection equals or exceeds some particular value  $x$  in the selected interval

$F(x)$  = probability that the deflection equals or exceeds some particular value  $x$ .

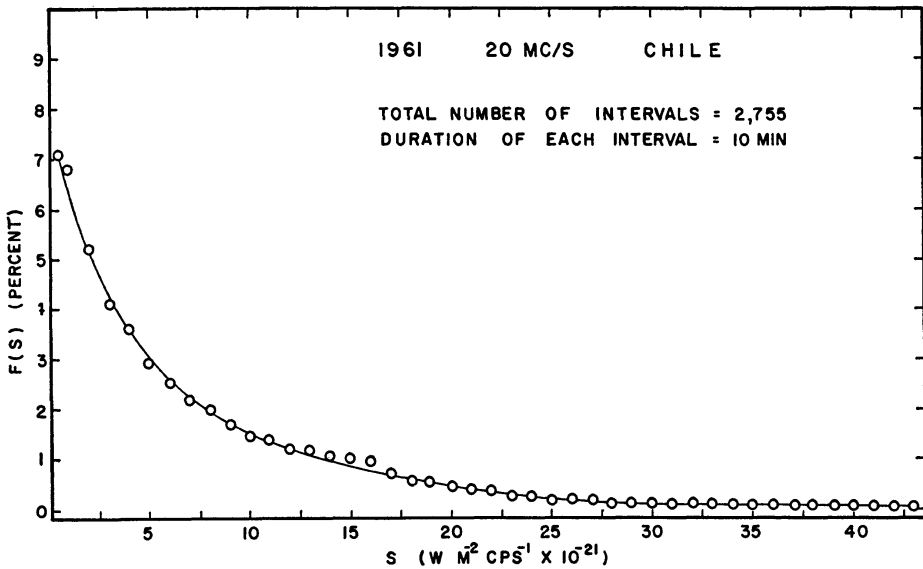


FIG. 8.—Probability distribution function for the peak flux densities in consecutive 10-min intervals, 20 Mc/s in Chile.

Calibrations indicated that the recorder deflection is approximately proportional to the square root of the radio-frequency power at the receiver input. Thus,

$$S = C (x_1^2 - x_0^2) \tag{6}$$

and

$$\langle S \rangle_1 = C (\langle x^2 \rangle - x_0^2), \tag{7}$$

so that

$$K = \frac{\langle x^2 \rangle - x_0^2}{x_1^2 - x_0^2}. \tag{8}$$

The deflections  $x_1$  and  $x_0$  are easily measurable. The determination of  $\langle x^2 \rangle$  for the interval was considerably more difficult; it was accomplished as follows.

The time  $t$  for which the deflection exceeded some particular value  $x$  during the selected interval of duration  $T$  was measured, and the ratio  $t/T$  was computed. This ratio is equal to  $F(x)$ . The measurement was repeated for other values of  $x$ , and  $F(x)$  was tabulated as a function of  $x$ . Since the time for which the deflection exceeds  $x$  is equal to the time for which its square exceeds  $x^2$ ,

$$F(x) = F(y), \tag{9}$$

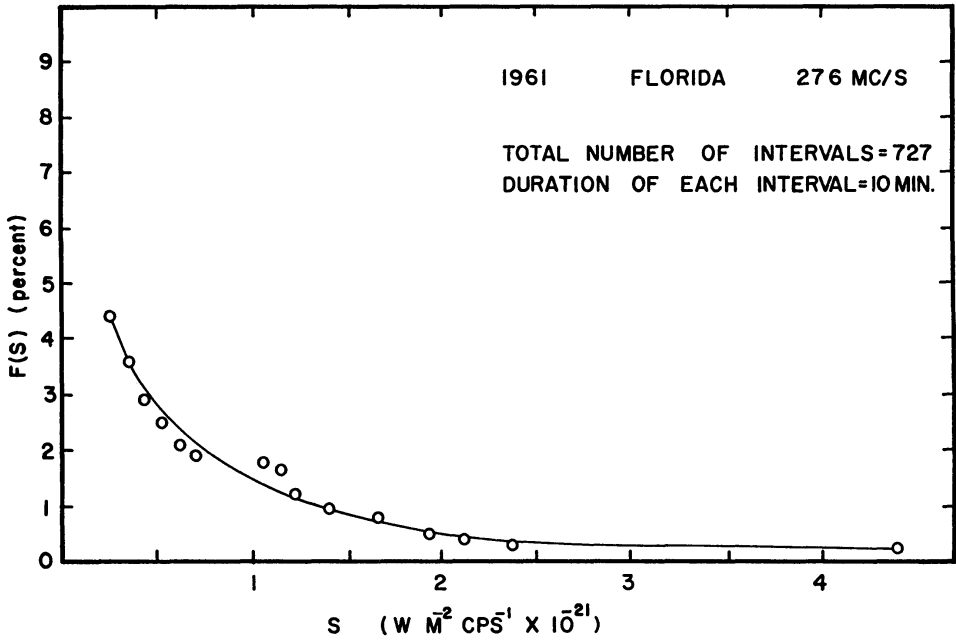


FIG. 9.—Probability distribution function for the peak flux densities in consecutive 10-min intervals, 27.6 Mc/s in Florida.

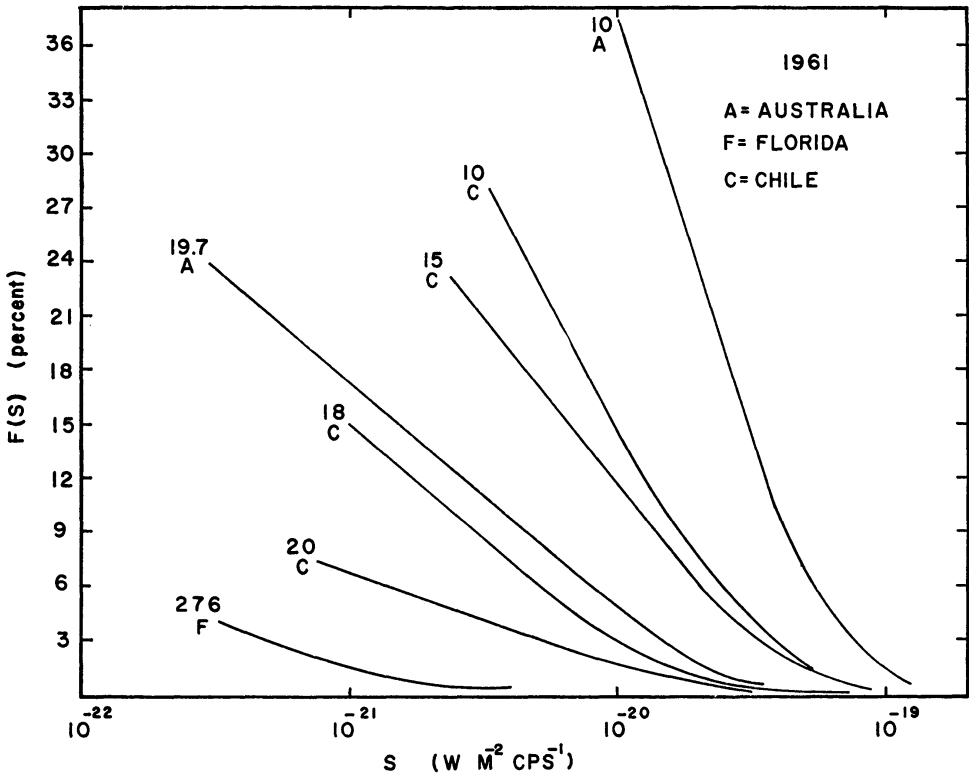


FIG. 10.—Semilogarithmic plot of all the distribution functions in Figs. 3-9. The frequency in megacycles and the observatory designation are indicated beside each curve.

where  $y = x^2$ . A tabulation of  $F(y)$  versus  $y$  was made from that of  $F(x)$  versus  $x$ . The probability that the square of the deflection lies between  $y$  and  $y + dy$  is  $f(y)dy$ , where

$$f(y) = -\frac{d}{dy}F(y). \quad (10)$$

Thus

$$\langle x^2 \rangle = \int_0^\infty yf(y)dy = \int_0^1 ydF(y) = \int_0^\infty F(y)dy. \quad (11)$$

The mean-square value of the deflection during the selected interval was thus determined by employing numerical integration to find the area under the curve of  $F(y)$  versus  $y$ .

The quantity  $K$  was first determined from recordings made at 15 Mc/s in Chile. Values were obtained for eight intervals of 10 min each. The intervals selected had been recorded on different nights, and were representative of a wide range of noise-storm intensities. The average of the 8 values of  $K$  at 15 Mc/s was 0.039; the standard deviation was 0.019.

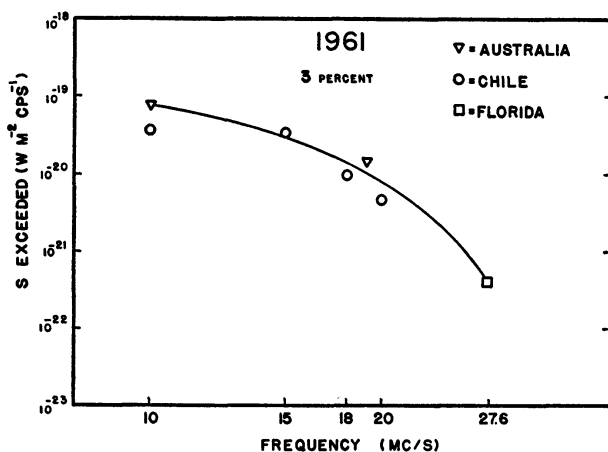


FIG. 11.—Flux densities which were exceeded in 3 per cent of the 10-min intervals, as a function of frequency.

Intervals of 1-min duration instead of 10 min were used in the investigation of the frequency dependence of  $K$  (designated  $K_1$  for 1-min intervals). About fifteen values of  $K_1$  were measured for each of five frequencies (except 27.6 Mc/s, for which only four measurements could be obtained). No more than one value per night was measured at a given frequency. The values of  $K_1$  for each frequency were averaged; the averages and the standard deviations are plotted in Figure 12. No significant variation of  $\langle K \rangle_1$  with frequency was found. It is therefore reasonable to conclude that there was also no significant variation of  $\langle K \rangle$  (for 10-min intervals) with frequency. It is interesting to note that  $\langle K \rangle_1$  is about  $2\frac{1}{2}$  times greater than  $\langle K \rangle$ . One would expect  $\langle K \rangle_1$  to exceed  $K$ , since smaller peak flux densities would be expected for 1-min intervals than for 10-min intervals.

A significant part of the structure of the observed noise bursts is believed to be due to the amplitude modulation by moving inhomogeneities in the terrestrial ionosphere of a more slowly varying signal arriving from Jupiter.<sup>1</sup> Such inhomogeneities are responsible for the scintillation of the continuously emitting discrete sources. The dimen-

<sup>1</sup> Observations made simultaneously in Florida and Chile during each Jovian apparition since 1960 have indicated little if any correlation between bursts having durations of the order of 1 sec (the most common type) at the two stations.

sions of those inhomogeneities producing most of the scintillations vary inversely with the wave frequency (Steinberg and Lequeux 1963). The results presented in Figure 12 suggest that the noise-burst shapes exhibit no marked frequency dependence between 10 Mc/s and 27.6 Mc/s. From this information, it should be possible to determine the distribution of the sizes of the inhomogeneities which are most effective in modifying the original Jovian burst structure.

It has been noted by a number of observers that the quality of the Jupiter noise as heard in the loudspeaker occasionally changes from the characteristic slow "swishes" to a series of rapidly repeated impulses somewhat similar to the radio noise caused by automobile ignition systems. This so-called "spitting" noise waxes and wanes irregularly, with periods of a few seconds. Oscillographic studies indicate that the individual impulses often recur at rates in the vicinity of 20 per second, and that the rise times are less than a millisecond, perhaps being limited by the receiver band width. Other relatively rare departures from the normal type of Jupiter burst are isolated sharp impulses, and long "rollers" of many seconds' duration. Obviously, average values of  $K$  for these exotic manifestations of Jupiter noise must be quite different from that for

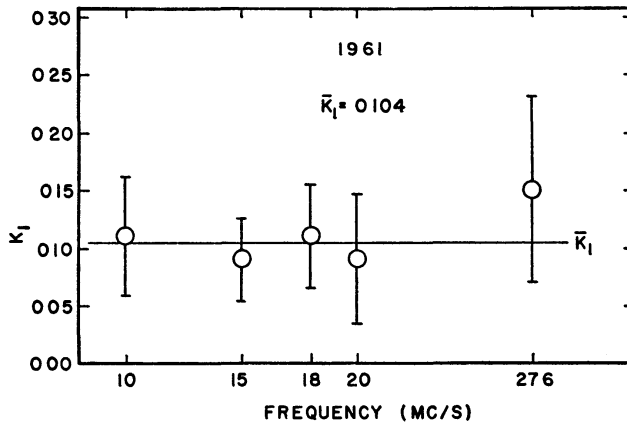


FIG 12.—Mean values of  $K_1$ , the ratio of the mean flux density to the peak flux density for 1-min intervals, plotted as a function of frequency. The heights of the vertical bars are twice the standard deviation.

the more usual type. No attempt was made to avoid the atypical bursts when intervals were selected for the determination of  $K$ . In a very few of the intervals selected, the noise was predominantly of the "spitting" type; however such cases were sufficiently infrequent that they produced negligible effect on the average value of  $K$ . This would have been true for any large sample of intervals selected at random.

#### IX. MEAN FLUX DENSITY AS A FUNCTION OF FREQUENCY

The mean (for the apparition) of the flux density at each frequency was found from equation (5), using the numerically computed integral of  $F(S)$  for that frequency, and the value of  $K$  determined in the preceding section. Unavoidable background-noise fluctuations prevented the measurement of  $F(S)$  for  $S$  closer to zero than certain limiting values. It was therefore necessary to extrapolate the curves of Figures 3-9 to zero  $S$  before the integrals could be found; straight-line extrapolations were employed. The mean values of Jovian flux density so determined are plotted as a function of frequency in Figure 13. Like the occurrence probability and the peak flux density, the mean flux density decreases monotonically with increase in frequency above 10 Mc/s. The ordinates of the dashed line drawn tangent to the plotted curve at 17 Mc/s are proportional to  $f^{-5.2}$ . The remarkably rapid decrease in the plotted curve with increase in frequency

results partly from the fact that noise bursts are generally weaker at the higher than at the lower frequencies, and partly from the fact that the occurrence probability is less at the higher frequencies. Figure 13 suggests that  $\langle S_a \rangle$  might attain a maximum at some frequency not far below 10 Mc/s.

#### X. THE INTEGRATED POWER FROM JUPITER

The area under the curve of  $\langle S_a \rangle$  versus  $f$  above 10 Mc/s is equal to the mean power per unit area (integrated flux density) reaching the earth from Jupiter at all frequencies above that value. Before the curve in Figure 13 could be integrated, it was necessary to extrapolate it to zero flux density at its high frequency end. A linear extrapolation was made from the value of  $\langle S_a \rangle$  on the curve at 27.6 Mc/s to  $\langle S \rangle_a = 0$  at 100 Mc/s. The exact location of the intercept is relatively unimportant, since the area under the extrapolated part of the curve is at least an order of magnitude less than that under the remainder. The integration was performed numerically. The value found in this

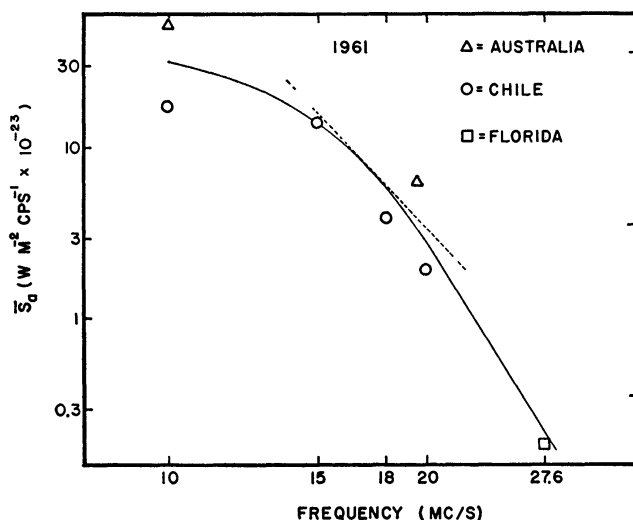


FIG. 13.—Mean flux density of the radiation from Jupiter in 1961 as a function of frequency (averaged over quiescent as well as over active periods). The dashed line represents the function  $(S_a) = Cf^{-5.2}$ , where  $C$  is a constant.

way for the mean integrated flux density for all frequencies above 10 Mc/s was  $2 \times 10^{-15} \text{ W m}^{-2}$ . If the curve in Figure 13 had been raised so that it passed through the two points from the Australian station, the value would have been about 60 per cent higher.

In order to arrive at an estimate of the mean integrated flux density from Jupiter at all frequencies in the decameter region, it was necessary to extrapolate the curve in Figure 13 to zero flux density at the low-frequency end, as well as at the high-frequency end. Since there is little on which to base such an extrapolation, the result may be subject to considerable error. However, by making two extrapolations, two values of integrated flux density were obtained which probably bracket the true value. In the first extrapolation, it was assumed that  $\langle S_a \rangle$  decreases linearly from  $3 \times 10^{-22} \text{ W m}^{-2} (\text{c/s})^{-1}$  at 10 Mc/s to zero at 2 Mc/s. The mean integrated flux density for all frequencies would then be  $3 \times 10^{-15} \text{ W m}^{-2}$ . In the other extrapolation,  $\langle S_a \rangle$  was assumed to increase linearly from  $3 \times 10^{-22} \text{ W m}^{-2} (\text{c/s})^{-1}$  at 10 Mc/s to five times this value at 5 Mc/s, and then to decrease linearly to zero at zero frequency. In this case the integrated flux density for all frequencies would be about  $10 \times 10^{-15} \text{ W m}^{-2}$ . Preliminary indications from the 1962 data are that  $\langle S_a \rangle$  at 5 Mc/s is not greatly different from

that at 10 Mc/s. It can therefore be stated with a fair degree of confidence that the average decametric power per unit area reaching the earth at all frequencies in 1961 was  $10^{-14} \text{ W m}^{-2}$ , to the nearest order of magnitude. If it is assumed that, on the average, power is emitted equally in all directions from Jupiter, the mean power of the decametric sources must have been about  $5 \times 10^{10}$  watts. This is 500 times the estimate made by Douglas and Smith (1963*b*) for frequencies above 5 Mc/s, and is an order of magnitude less than that made by Gallet (1961). It should be pointed out that the estimates of Douglas and Smith and of Gallet were based on much less certain data for the lower frequencies than is the present estimate. If the decametric radiation is not emitted equally in all directions, on the average, then the mean power might be either higher or lower than the estimate above, depending upon the relative probability of emission toward the earth.

It is generally believed that the solar wind powers the sources of both the decameter radiation and the non-thermal component of the decimeter radiation. The flux density of the latter is almost constant, being about  $6 \times 10^{-26} \text{ W m}^{-2} (\text{c/s})^{-1}$ , over an observed frequency range of some 5000 Mc/s (Gower 1963). This corresponds to an integrated flux density of about  $3 \times 10^{-16} \text{ W m}^{-2}$  for the decimeter radiation, which is almost two orders of magnitude less than the value given above for the decameter radiation.

In order to obtain some idea of the over-all efficiency of the decametric emission process, we must estimate the power intercepted by Jupiter from the solar wind. Results from the space probes Pioneer V, Explorer X, and Mariner 2 have indicated that in the vicinity of the orbit of the earth, the quiet solar wind contains about 10 ion pairs per cubic centimeter, traveling with a speed of about 400 km/sec (Snyder, Anderson, Neugebauer, and Smith 1962). This corresponds to a kinetic power flux of  $5.3 \times 10^{-4} \text{ W m}^{-2}$ . Assuming an inverse-square dependence upon distance, the kinetic flux at the orbit of Jupiter would be about  $2 \times 10^{-5} \text{ W m}^{-2}$ . The solar-wind power flowing normally through an area of about  $0.5R_J^2$  would then be equal to that of the decametric radiation,  $R_J$  being the radius of Jupiter. Studies of that component of the decimeter radiation which is due to synchrotron emission indicate that the magnetic field near Jupiter's surface at the equator is in the vicinity of 20 gauss. If Jupiter's field were not rotating, and if the flow of the solar wind were still laminar at Jupiter's orbit, then the magnetospheric envelope would be teardrop-shaped, with a stagnation point at the front. Assuming the energy density of the solar wind at Jupiter's orbit to be about  $\frac{1}{25}$  that at the orbit of the earth, the distance of the stagnation point from the center of the planet is about  $60R_J$ , according to the relation given by Axford (1962). Actually, however, the rotation of the field must exert a great influence on the boundary location. If we disregard the solar-wind velocity and assume that Jupiter is rotating in a sea of stationary plasma, the plasma will possess an apparent circulatory motion relative to the field. At the magnetospheric boundary, the apparent kinetic energy density of the plasma must be approximately equal to the magnetic energy density, so that

$$\frac{R}{R_J} = \left( \frac{H_e}{\omega R_J} \right)^{1/4} (4\pi n m_p)^{-1/8}, \quad (12)$$

where  $R$  is the approximate distance from the center of the planet to the magnetospheric boundary in the equatorial plane,  $H_e$  the equatorial magnetic field at the Jovian surface,  $\omega$  the angular velocity of rotation,  $n$  the number density of protons, and  $m_p$  the mass of a proton. A similar relation has been derived by Ellis (1963). If  $n$  at Jupiter's orbit is  $0.4 \text{ cm}^{-3}$ , then  $R$  as calculated by equation (12) is about  $50 R_J$ , which is close to the value obtained for the model of a non-rotating planet in a laminar solar-wind flow. Although the actual situation is much more complicated than either of these models, it nevertheless seems reasonable to assume that the radius of the magnetospheric cross-section perpendicular to the direction of solar-wind flow is about  $50 R_J$ , and the



area is about  $8000 R_{\odot}^2$ . From the power of the solar-wind particles impinging upon this area, we conclude that the efficiency of energy conversion from the solar wind to decimeter radiation was of the order of  $10^{-4}$  in 1961, if only the quiet solar wind is considered; however, since the solar-wind power must often have risen above its undisturbed value, the true efficiency was probably closer to  $10^{-5}$ .

#### XI. JUPITER'S COMPLETE RADIO SPECTRUM

Some idea of the relationship between the three regions of Jupiter's radio spectrum which have been recognized as distinct is given by Figure 14. The solid lines in the decameter region are the curves for peak and average flux density, taken from Figures 2 and 13, respectively. The solid line in the decimeter region represents a mean of the published data (Gower 1963). Although the spread in the reported measurements is

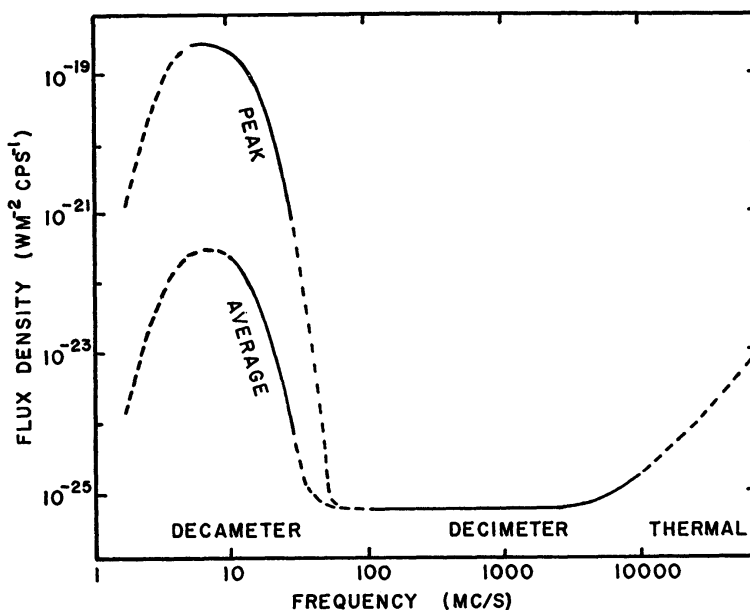


FIG. 14.—Suggested appearance of Jupiter's radio spectrum above 1 Mc/s. The curve marked "average" represents the variation of mean flux density with frequency during the 1961 apparition; the one marked "peak" represents the average of the five highest nightly maximum flux densities at each frequency during the 1961 apparition. The curve above 100 Mc/s was plotted from data summarized by Gower (1963). No observations have been made in the regions indicated by the dashed curves, which should be regarded as conjectural.

rather large, no significant variation of flux density with frequency between 178 and 3000 Mc/s has yet been found. Flux densities at 10000 Mc/s and at infrared frequencies are close to the values one would expect if Jupiter emits as a black body at  $130^{\circ}$  K (Roberts 1963). The dashed curves in Figure 14 are, of course, conjectural.

It is important that measurements be extended to the parts of the spectrum indicated by the dashed curves. The low-frequency extremity, at which observations have so far been impossible because of ionospheric opacity, is perhaps the most interesting of the unexplored regions. It seems likely that 5 Mc/s is about the lowest frequency at which measurements of flux density and occurrence probability can be made from terrestrial observatories over extended periods, although occasional observations can no doubt be made at somewhat lower frequencies. Even at 5 Mc/s, good measurements are extremely difficult to obtain, being possible only during the years of minimum solar activity, and then only for 2 or 3 hours before dawn under circumstances for which

Jupiter is not far from zenith. Tests conducted at the Maipu Radioastronomical Observatory in 1962 indicated that much of the terrestrial interference, which is particularly severe at the lower frequencies, can be eliminated by the proper choice of the antenna site.<sup>2</sup> The full exploration of the region below 5 Mc/s, however, will have to await the development of a suitable radio telescope which orbits above the ionosphere.

Observations are also needed at some frequency in the meter wavelength range with a radio telescope having sufficient sensitivity to detect both the bursts characteristic of the decameter radiation and the continuum characteristic of the decimeter radiation. Occasional detection of bursts should be possible at 40 Mc/s with the 1000-foot dish at the Arecibo Ionospheric Observatory. However, the detection and measurement of the continuum at this frequency will probably be more difficult because of the high brightness temperature and complicated structure of the galactic background.

We wish to thank Mr. O. B. Slee for providing the 85.5 Mc/s data and for his assistance in many other ways; Dr. J. A. Roberts for helpful discussions in connection with the work; and Dr. N. F. Six for his assistance in reducing the data. We also wish to acknowledge the encouragement and the valuable suggestions of the late Dr. J. L. Pawsey. We gratefully acknowledge the financial support of the U.S. National Science Foundation, the Office of Naval Research, and the Army Research Office (Durham).

#### REFERENCES

- Axford, W. I. 1962, *J. Geophys. Res.*, **67**, 3791.  
 Carr, T. D. 1958, thesis, University of Florida.  
 Carr, T. D., Smith, A. G., Bollhagen, H., Six, N. F., Jr., and Chatterton, N. E. 1961, *Ap. J.*, **134**, 105.  
 Douglas, J. N. 1960, thesis, Yale University.  
 Douglas, J. N., and Smith, H. J. 1963a, *A.J.*, **68**, 163.  
 ———. 1963b, *La Physique des planetes* (Liège: Cointe-Sclessin), p. 551.  
 Ellis, G. R. A. 1962, *Nature*, **194**, 667.  
 ———. 1963, *Australian J. Phys.*, **16**, 74.  
 Gallet, R. M. 1961, *Planets and Satellites*, ed. G. P. Kuiper and B. M. Middlehurst (Chicago: University of Chicago Press), p. 525.  
 Gardner, F. F., and Shain, C. A. 1958, *Australian J. Phys.*, **11**, 55.  
 Gower, J. F. R. 1963, *Nature*, **199**, 1273.  
 Kraus, J. D. 1958, *Proc. I.R.E.*, **46**, 273.  
 Mills, B. Y., Little, A. G., Sheridan, K. V., and Slee, O. B. 1958, *Proc. I.R.E.*, **46**, 67.  
 Roberts, J. A. 1963, *Planet. and Space Sci.*, **11**, 221.  
 Shain, C. A. 1958, *Proc. I.R.E.*, **46**, 85.  
 Six, N. F., Jr. 1962, thesis, University of Florida.  
 Smith, A. G., Carr, T. D., and Chatterton, N. E. 1963, *Proc. 12th International Astronautical Congress* (New York: Academic Press), p. 689.  
 Snyder, C., Anderson, H. R., Neugebauer, M., and Smith, E. J. 1962, *University Conference on Space Exploration, Chicago* (Proc. NASA) (Washington, D.C.: Government Printing Office), p. 179.  
 Steinberg, J. L., and Lequeux, J. 1963, *Radio Astronomy* (New York: McGraw-Hill Book Co.), p. 9.  
 Warwick, J. W. 1963, *Ap. J.*, **137**, 41.

<sup>2</sup> Simultaneous pre-dawn observations were made for a total of 62 hours with a 10 Mc/s array at an exposed location at the Maipu Radioastronomical Observatory and with an identical array on the floor of a deep canyon 650 km to the north. The latter array was situated in the geometrical shadow of the canyon walls for all rays arriving at elevation angles less than about 45°. Terrestrial interference remained at a low enough level for satisfactory monitoring of Jupiter 55 per cent of the observing time at the canyon site, but only 5 per cent of the time at the Maipu site.